Journal of Power Sources 196 (2011) 1833–1839

Contents lists available at ScienceDirect

Journal of Power Sources

journal homepage: www.elsevier.com/locate/jpowsour

Estimation of hydrogen crossover through Nafion® membranes in PEMFCs

Carlotta Francia*, Vijaykumar S. Ijeri, Stefania Specchia, Paolo Spinelli

Department of Materials Science and Chemical Engineering, Politecnico di Torino, Corso Duca degli Abruzzi 24, 10129 Torino, Italy

ARTICLE INFO

Article history:
Received 19 July 2010
Received in revised form 31 August 2010
Accepted 21 September 2010
Available online 1 October 2010

Keywords:
Hydrogen crossover
Semi-empirical model
Nafion membranes
Fuel cells

ABSTRACT

It is well known that the membrane electrode assembly (MEA) of proton exchange membrane fuel cells (PEMFCs) can undergo deterioration, during long term operation, of both the electrode materials and the membrane. Hydrogen crossover, i.e., the undesired diffusion of the gas from the anode to the cathode through the membrane, has been ascribed as one of the main causes of deterioration of perfluorinated ionomer membranes, normally employed in PEMFCs. One of the effects of the hydrogen permeation across the membrane is the decrease of the cell's open circuit voltage (OCV), due to the reaction between the fuel and the oxidant at the cathode surface. Such reaction can lead to the production of peroxide radicals, causing the degradation of both the PEM and the catalyst layer. Hydrogen crossover increases when temperature, pressure and humidity of the cell rise. The hydrogen permeation rate through a very thin PEM is typically lower than 1 mA cm^{-2} for a new MEA, but it can exceed 10–20 mA cm^{-2} after long term operation. Various methods have been proposed to measure the rate of hydrogen crossover, mainly based on electrochemical tests on a single FC with a flow of nitrogen at the cathode, so that the steady state current corresponds to the oxidation of crossed hydrogen. Hydrogen crossover has been also determined indirectly by assuming that the changes in the OCV values are due to the passage of fuel from the anode to the cathode.

In this paper, a simplified mathematical model for the direct determination of hydrogen crossover permeation rate is presented. Such a model is based on analytical expressions of the polarization terms and it is employed to determine the hydrogen crossover rate. The main results show that the hydrogen crossover current densities increased from 0.12 to 0.32 mA cm^{-2}, by decreasing the thickness of the membranes and increasing the operating cell temperature. Moreover, the hydrogen crossover determined for a fresh MEA was compared with that of a degraded one, exposed to repetitive freezing/thawing cycles. It was found that the hydrogen crossover for the degraded MEA was more than twice the value obtained with the fresh one at the same temperature.

1. Introduction

With hydrogen being contemplated as the fuel of the future, fuel cells (FCs) play an important role in such a hydrogen economy. Hydrogen based polymer electrolyte fuel cells (PEMFCs) can help in reducing our dependence on fossil fuels and diminish toxic emissions into the atmosphere since water is the final product of the reaction. Moreover, PEMFC vehicles using pure hydrogen as fuel are of great interest as the FC itself has an efficiency of almost 50% and with appropriate heat recovery systems it could reach 80% [1–3].

The two major hurdles limiting the large scale commercialization of PEMFCs are the cost and durability. It is necessary for the FC power system to cost less than 50$ kW^{-1} to be technologically competitive and the target for 2015 is 30$ kW^{-1} [1,4]. Two main approaches in this direction have been the reduction of the Pt loading through dispersion on various carbon supports [5,6] and the use of non-noble metal catalysts [7].

The durability of FC systems operating under automotive conditions has not been established yet. FC power systems will be required to be as durable and reliable as current automotive engines (i.e., 5,000 h lifespan or 150,000 miles equivalent) and able to function over the full range of external environmental conditions (−40 to +40 °C) [4]. Several factors affect the durability of PEMFCs, like catalyst layer degradation [8], gas diffusion layer degradation [9], carbon support corrosion [10], and degradation of the polymeric membrane [11–14].

The membrane accounts for a substantial portion of the FC costs (about 6%) [1]; since its durability is interconnected with the overall cost of its operation, it becomes important to study the causes that lead to degradation of the membrane. Nafion®, a sulfonated perfluoro polymer, is probably the most studied and employed electrolyte for PEMFC but other perfluorocarbon sulfonic acid membranes from Dow, Gore and Asahi Chemical were also used and investigated [3].

* Corresponding author. Tel.: +39 011 0904638; fax: +39 011 0904699.
E-mail address: carlotta.francia@polito.it (C. Francia).

0378-7753/$ – see front matter © 2010 Elsevier B.V. All rights reserved.
doi:10.1016/j.jpowsour.2010.09.058

The membrane serves as a barrier between the anode and the cathode, and aids proton conduction while being an electron insulator. It is normally assumed that the membrane is impermeable to gases. But there is always some amount of gases which move within the membrane and reach the other side. So, when oxygen and hydrogen permeate through the membrane and react directly with each other, the energy is lost as heat. This leads to the inefficiency of the FC. In addition, such gas crossover leads to the formation of peroxide and hydroperoxide radicals which cause further deterioration of the membrane [15,16].

Chen et al. [17] treated Nafion® membranes with Fenton's reagent and analyzed by X-ray photoelectron spectroscopy; a clear evidence of polymer degradation was observed. Fenton's reagent is a well-known source of hydroxyl radicals, and the similarity between the *in situ* (FC operation) and *ex situ* (Fenton's test) degradation mechanism was reported earlier [18,19]. Exposure of the membrane to 2 h of X-ray radiation did not affect the chemical structure of the membrane, however, treatment with Fenton's reagent indicated that the $(CF_2)_n$ polymer backbone had decomposed [17]. Fluorine and sulfur XPS peak intensity decreases were consistent with the detection of fluoride and sulfate ions during FC tests. The increase in oxygen atom concentration suggested oxygen-rich moieties formed in the membrane. These results indicated that in addition to degradation of the polymer side chain, chemical attack of the CF_2 backbone could be the primary reason for extensive fluorine loss and hydrogen crossover in membranes after long-term operation. It was suggested that degradation occurred mainly within the membrane or at the membrane–electrode interface [17].

Takaichi et al. [20] have shown that the gas permeation coefficient of hydrogen in Nafion® is nearly twice that of oxygen and it increases with increasing the relative humidity. They also demonstrated the distribution profiles of hydrogen and oxygen permeating in the PEM by monitoring the mixed potential, determined by the ratio of permeated hydrogen and oxygen.

Liu et al. [21] studied the ageing mechanisms of Nafion® 112 membranes under cyclic as well as constant current loading conditions. Under cyclic conditions, it was seen that hydrogen crossover increased dramatically after 500 h of current cycling due to pinhole formation and that was the most dominant degradation source. The FC approached the end of its useful lifetime after 1,000 h of operation. On the other hand, the hydrogen crossover rate remained approximately constant for the membrane under constant current operation. The OCV of the cyclically aged membrane remained at about 0.9 V until 500 h after which, it decreased almost linearly. The membrane under constant current load, showed a very low crossover with an OCV of about 0.9 V over the period of 1,000 h. Thus the decrease in OCV correlates with the crossover of hydrogen. Moreover, the increase in hydrogen crossover also causes a decrease in the electro-active surface area of the catalyst [22]. Recently the interest in hydrogen crossover for PEMFCs markedly increased due to the strong connection between this phenomenon and the mechanism of membrane degradation [23–26].

A FC operation presents a complexity of variables for its performance and durability. So it becomes important to develop mathematical models to extract and/or predict the parameters for long term reliable operations. Liu et al. [21] used phenomenological modeling with values of ageing parameters substituted into the semi-empirical FC performance equations to explain the observed ageing phenomena and predict the cell behavior at different time periods. The exchange current density was utilized as the sole adjustment parameter during the modeling process. The model-predicted trends provided good fits to experimental data for the membrane under constant current ageing conditions but the experimental voltage profile was found to have a large phase lag behind the predicted one for the membrane under cyclic ageing conditions. A model for numerical analysis of gas crossover through the membrane in PEMFCs developed by Seddiq et al. [27] concluded that the direct reaction between hydrogen and oxygen increases with a decrease in thickness of membrane, and that it mainly occurs at the cathode at low current density conditions. More sophisticated modeling approaches have been presented by Sompalli et al. [28] by considering the impact of electrode overlap on membrane degradation, and by Nam et al. [29] who presented a numerical gas crossover model, including non-isothermal and two-phase conditions.

As previously indicated, the strong correlation between the open-circuit voltage (OCV) and hydrogen crossover through the membrane in low temperature PEMFCs has been the object of numerous papers dealing with MEAs degradation, see, e.g., Vilekar and Datta [30] and references therein. It is now accepted that the OCV values in such systems correspond to a mixed potential condition at the oxygen electrode, due to the very low value of the exchange current density for the ORR. The above paper [30] represents an extensive approach to the subject, encompassing the theoretical background of this complex situation.

Direct measurement of the hydrogen crossover current can be obtained by LSV tests in single PEMFC with hydrogen fed to the anode side and nitrogen fed at the cathode. In the potential range from 0 to 0.6 V vs. the anode, the limiting hydrogen oxidation current corresponds to the hydrogen crossover rate [31]. This technique has been frequently used in membrane degradation studies [14,24–26]. Other methods involve direct hydrogen permeability tests through the membrane [32]. Due to the difficulty in direct determination of hydrogen crossover, other approaches have been proposed by taking into account the OCV change following the oxidation of crossed hydrogen at the oxygen electrode. This evaluation is based on the assumption of a mixed electrode potential at the cathode involving the electrochemical reduction of oxygen and the oxidation of hydrogen passing through the membrane. Considering this interpretation, a semi-empirical approach has been previously proposed by the authors [33]. The simplified mathematical model, based on analytical expressions of the polarization terms, was employed to determine the hydrogen crossover permeation rate, together with the evaluation of the electro-catalytic activity. The novelty of the present approach is that the hydrogen crossover current is obtained by best-fitting the initial part of the polarization curve, therefore separate electrochemical tests for this determination are not required. In addition, the complete analysis of the polarization curve provides all the significant parameters for the cell performance. This can result in a simpler experimental approach to the investigation of PEMFC degradation.

This study investigates the applicability of the semi-empirical approach to the phenomena of H_2 crossover in PEMFCs. The analysis is focused on Nafion® membranes of different thickness, namely Nafion® 112, 115 and 117, and at three different temperatures, 60, 70 and 80 °C, respectively. As it is required for a FC to operate over a range of temperatures [1], some membranes were subjected to various freezing/thawing cycles [34–36] and also tested to evaluate the hydrogen crossover rate in degraded MEAs. The simplified mathematical model based on Butler–Volmer equation for the electrochemical kinetics of hydrogen and oxygen reactions is proposed to analyze the polarization curves of single PEMFCs by computing the different overpotential components, which provide the best fitting of the experimental data. The OCV for the oxygen electrode, which is known to be markedly lower than the reversible potential, was interpreted in terms of mixed potential, assuming an arbitrary parasitic oxidation reaction that corresponds to hydrogen crossover. The fitting of the experimental polarization data allowed a very good estimation of the hydrogen crossover rate, as a function of the membrane thickness and the cell operation temperature.

2. Experimental

All the tests were carried out in a 5 cm^2 single PEMFC (Electrochem Inc.) with serpentine patterns. A standard procedure for the MEA preparation was set up, which was developed in our laboratory [37]. The catalyst ink, obtained by mixing the standard Pt catalyst (20 wt.% Pt on Vulcan XC-72R, ElectroChem Inc) with Nafion® ionomer (5 wt.% solution, EC-NS-05, ElectroChem Inc.), isopropyl alcohol (Aldrich) and water, was painted on a LT 1200-W ELAT gas diffusion layer (E-TEK). The Pt load was fixed at the value of 0.5 mg cm^{-2} on both the anode and the cathode sides. The MEAs were prepared with three different commercial polymer membranes (Ion Power, Inc.): Nafion® 117 (thickness ~180 μm), Nafion® 115 (thickness ~130 μm) and Nafion® 112 (thickness ~50 μm), by hot pressing the electrodes to the membrane at 110 °C. Low precision glass silicon rubber gaskets (Electrochem Inc.) were used in the FC. The cell was assembled with the retaining bolts torque set at 1.5 N m.

Analyses were carried out with a purposely designed test bench for small single PEMFC [33]. The MEAs underwent the same conditioning procedure in order to equilibrate the water content into the Nafion® membrane. The PEMFC was fed with humidified pure hydrogen and oxygen at the temperature of 80 °C. During conditioning, the FC was kept at the constant voltage of 0.5 V for 8 h.

The polarization curves of the FC were obtained by a slow potentiodynamic technique by means of an AMEL potentiostat MOD 7050. The current intensity was recorded by varying the cell voltage at a low scan rate (0.2 mV s^{-1}) from the OCV to 0.5 V and reverse. The polarization curves were traced at three different cell temperatures (60, 70 and 80 °C) for the different MEAs.

By considering previous studies of the authors related to the degradation effects on MEAs exposed to repeated freezing/thawing cycles [34,35] the most aged MEA, prepared with Nafion® 112, was employed to evaluate the hydrogen crossover and to study how the MEA degradation could affect the hydrogen crossover rate. Briefly, the Nafion® 112 MEA specifically used for this purpose was repetitively subjected to 20 freezing/thawing cycles from −10 to +20 °C, for a total of approx. 50 h of discontinuous work under load. Before each freezing/thawing cycle, the Nafion® 112 MEA was first tested at 80 °C and then purged with dry air on both sides to remove the water formed during electrochemical reactions. The water present in the cell, in fact, can freeze and lead to ice formation, with a consequent permanent damage of the PEMFC [38–40].

The morphological structure of the tested MEAs was investigated by employing a scanning electron microscope (SEM FEI QUANTA INSPECT LV 30 kV). Cross-sections of the MEAs were prepared by freeze-fracturing the entire assembly, previously pre-cut with scissors, after immersion for 10 min in liquid nitrogen.

3. Results and discussion

For each prepared MEA (Nafion® 117, 115 and 112) and each operating condition (cell temperatures of 60, 70 and 80 °C), three runs were carried out to check the test reproducibility. Fig. 1 shows an example of the polarization curves traced on the Nafion® 112 MEA at 60 °C. A very good reproducibility was found both at high and at low current densities (*see* the semi-logarithmic plot in the box of Fig. 1).

The analysis of the polarization curves by the semi-empirical model [33] allows the determination of the hydrogen crossover rate together with other important parameters for evaluating the electro-catalytic activity and the MEA performance. It is known that the measured OCV of single PEMFC markedly differs from the value computed according to the equilibrium (Nernst) equation. Such a difference is attributable to the oxygen electrode, for

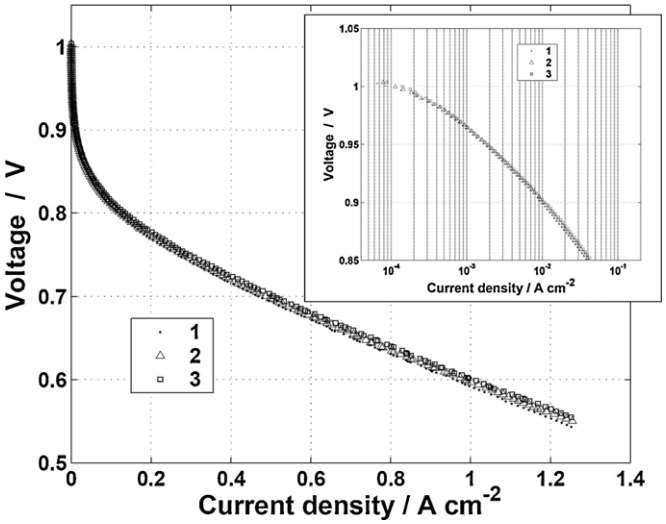

Fig. 1. Plot of three polarization curves obtained with a 5 cm^2 Nafion® 112 MEA under the same conditions to check the reproducibility. Pt load 0.5 mg cm^{-2}, humidified hydrogen and oxygen (100% RH), at atmospheric pressure, stoichiometry flow 2, temperature 60 °C. The inset shows the low current region on the semilogarithmic plot.

which equilibrium conditions cannot be attained at open circuit. From the basic studies by Tarasevich et al. [41], Damjanovic et al. [42] and Hoare [43], the reasons for this behavior were interpreted in terms of parasitic reactions responsible for a mixed-potential condition. Among the various parasitic reactions which have been assumed to explain the attainment of the mixed potential, those which received major attention are Pt oxidation, organic impurities oxidation, and hydrogen peroxide reactions. In PEMFCs, in addition to such parasitic reactions, which occur independently of the hydrogen electrode, the major effect on the open circuit potential is related to the small amount of hydrogen crossing the membrane, which is rapidly oxidized at the cathode, resulting in the so-called hydrogen crossover current. In the present approach, such phenomena were accounted for, by assuming an arbitrary oxidation current which should include all possible causes. This is schematically illustrated in Fig. 2, where the fitting of experimental data at low current densities was obtained by using such an empirical approach. The test in Fig. 2 refers to the polarization curve obtained

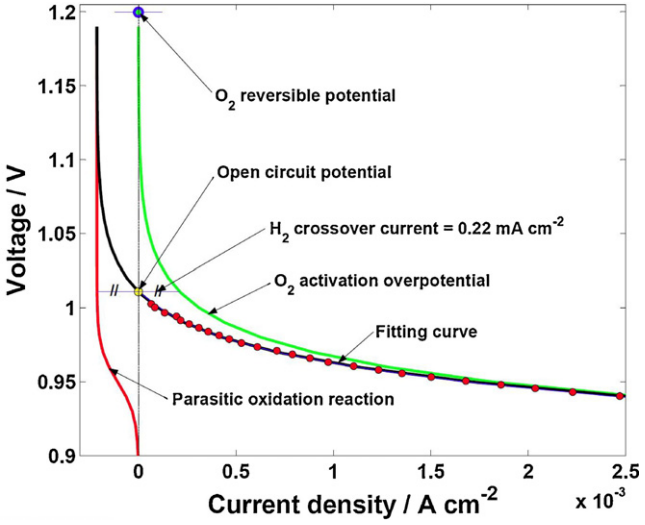

Fig. 2. Mixed potential analysis of the polarization curve. The test refers to a 5 cm^2 Nafion® 112 MEA at 60 °C. The closed circles are the experimental points.

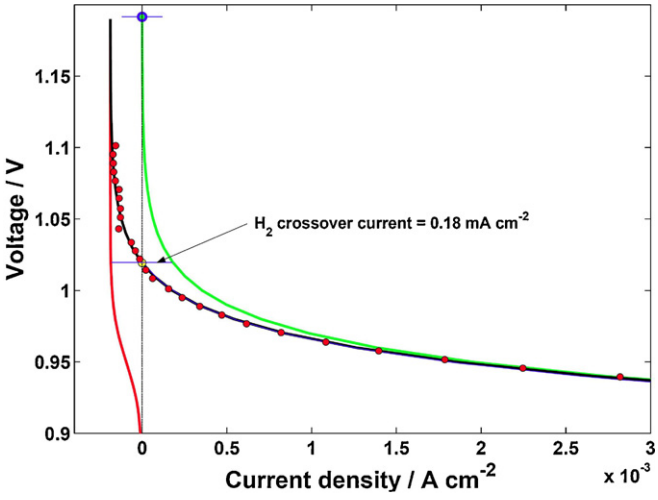

Fig. 3. Mixed potential analysis for a 5 cm² Nafion® 117 MEA at 70 °C. The experimental points were obtained extending the polarization by about 80 mV above the OCV to confirm the validity of the analysis.

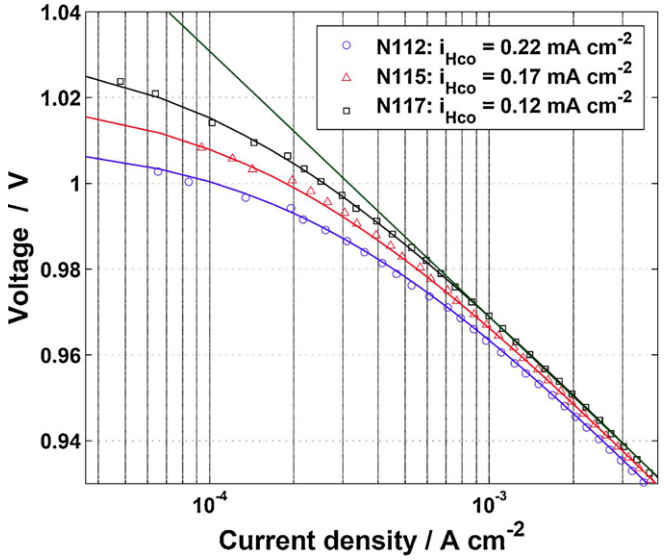

Fig. 4. Semilogarithmic plot of polarization curves carried out with three different MEAs (Nafion® 112, 115 and 117) at 60 °C. The straight Tafel line for oxygen reduction is plotted for the Nafion® 117 MEA.

at 60 °C with a MEA prepared with Nafion® 112. On the graph, the circles refer to the experimental points; the FC reversible voltage and the OCV due to the mixed potential are also shown. The anodic curve corresponding to the "parasitic oxidation reaction" was chosen according to the following equation:

$$V_s = V_{s0} + c_s \frac{RT}{F} \log\left(\frac{I_s}{I_{ls} - I_s}\right) \quad (1)$$

where V_s and I_s are the voltage and current values for the parasitic reaction(s), and V_{s0}, c_s and I_{ls} are empirical parameters to be obtained by the best-fitting procedure described further on. It can be noted that V_{s0} can be interpreted as the half-wave potential of the anodic curve, while I_{ls} corresponds to the limiting current value for the oxidation reaction. The computed curve resulting from the algebraic sum of equation (1) and the Butler–Volmer equation for ORR is obtained by best-fitting of the experimental points in the low current density region (typically <2.5 mA cm^{-2}), where all the other dissipation terms are negligible (for a discussion of this assumption, see Ref. [33]). The result of the best-fitting also provides a very good estimation of the OCV. The value of the current density for the parasitic reactions at the open circuit potential is taken as the hydrogen crossover rate. In fact, this current is mainly due to the oxidation of hydrogen permeating the membrane, the other oxidation reactions being negligible. This result is confirmed by the values of the hydrogen crossover rates determined by other methods [31]. For some tests with Nafion® 117 MEA, a confirmation was also obtained by slightly extending the polarization curve above the OCV. This is illustrated in Fig. 3 where the data of a Nafion® 117 MEA at 70 °C are shown. The experimental points include a small region above the OCV, for which the very good agreement between the fitting curve and the experimental points is also demonstrated. It is worth noting that a polarization above the OCV means an inversion of the cell condition: the cell becomes an electrolyzer. This condition must be limited to a very small polarization to reduce possible negative effects on the catalyst.

The results of all the performed tests indicated values of the hydrogen crossover current densities ranging from 0.22 to 0.32 mA cm^{-2} for the Nafion® 112 MEA, in the chosen temperature range. For Nafion® 115 and Nafion® 117 MEAs, lower values were obtained, as expected by considering the greater membrane thickness, showing a corresponding increase with temperatures. The lowering of the crossover values with the increase of the membrane thickness can be related to the decrease of the hydrogen concentration gradient within the membrane [44]. The results are summarized in Table 1.

An example of the potentiality of the proposed method is shown in Fig. 4, where the comparison of the three different membranes at the temperature of 60 °C is illustrated. Again, the experimental polarization curves were analyzed according to the above described method and the corresponding values of the hydrogen crossover current densities were obtained. The graph is in the form of semilogarithmic plots, thus the values at very low current density are more readable. The straight line is the Tafel-line for oxygen reduction in the case of Nafion® 117 MEA. It can be seen that the more the experimental curve diverges from the straight line, the higher is the hydrogen crossover current density; correspondingly a lower OCV was observed.

To confirm the interest of the present approach as a tool to investigate the MEA degradation, the hydrogen crossover current was determined on a Nafion® 112 MEA which was subjected to 20 freezing/thawing cycles, herein after named degraded MEA. The analysis of the polarization curve carried out at 80 °C on the degraded MEA provided a value of the hydrogen crossover current density of 0.73 mA cm^{-2}, which is more than twice the value obtained with

Table 1
Hydrogen crossover current densities (mA cm^{-2}) and OCV values (V) for Nafion® 112, Nafion® 115 and Nafion® 117 MEAs at various operating cell temperatures.

Nafion® membrane	Temperature (°C)					
	60		70		80	
	I_{H_2} (mA cm^{-2})	OCV (V)	I_{H_2} (mA cm^{-2})	OCV (V)	I_{H_2} (mA cm^{-2})	OCV (V)
117	0.12	1.024	0.19	1.014	0.24	1.011
115	0.17	1.019	0.21	1.013	0.27	1.002
112	0.22	1.011	0.25	1.008	0.32	0.996

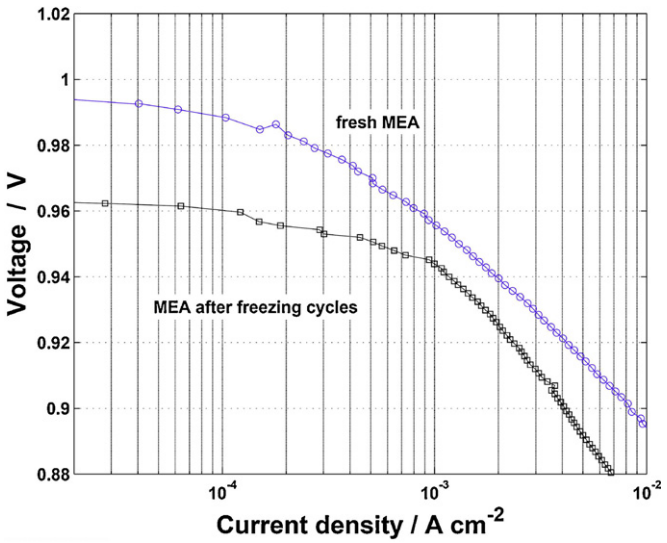

Fig. 5. Semilogarithmic plot of polarization curves at 80 °C obtained with the fresh Nafion® 112 MEA and with the degraded one.

the corresponding fresh Nafion® 112 MEA (0.32 mA cm^{-2}) at the same temperature. Fig. 5 plots the comparison of the polarization curves of the fresh Nafion® 112 MEA and the degraded one. A remarkable decrease of the OCV for the degraded MEA was noticed, which was consistent with the increase of the hydrogen crossover current.

A comparison of the SEM images of the cross-sections of the degraded MEA and of a fresh Nafion® 112 MEA (i.e., a prepared MEA never used) is shown in Fig. 6, where a notable morphology change of the membrane can be observed. In particular, for the new MEA (Fig. 6A and C), the adhesion between the highly porous, catalytic layer and the membrane was perfect, without any area of delamination or fracture. The membrane itself appeared quite compact, without any sign of deterioration. But, in the cross-sections of the degraded MEA (Fig. 6B and D), the membrane appeared altered compared to the fresh one, with the presence of creeps (which are known in literature to affect the ohmic resistance, i.e., the power density decay [45]) and an increased roughness, while the morphology of the catalyst layer appeared to be the same as the fresh counterpart, even if the catalytic layer was slightly detached in some CL/PEM areas (see Fig. 6B). Moreover, a significant thinning of the membrane was noticed all along the MEA; while the fresh membrane measured approximately 50 μm, the thickness of the degraded one was reduced to approximately 40 μm. In literature, the membrane thinning is known to be a direct consequence for the increasing of H_2 crossover [23,26,44,46,47]: it has been shown, in fact, that degradation rate is dependent on initial membrane thickness. In turn, a thinner membrane causes a higher hydrogen crossover rate. Yuan et al. [23] tested a 4-cell stack for 1,000 h under idle conditions to measure the membrane degradation of each cell: the thinner membranes displayed more rapid rates of degradation than thicker. This degradation was caused by hydrogen crossover, which indicated membrane thinning and holes formation. The membrane thinning may be occurred by chemical attack of hydrogen peroxide formed by electrochemical reaction of oxygen and hydrogen crossed over through the membrane [19,24,47,48]. For example, Oono et al. [49] localized by SEM inspections some holes in the cell membrane after long term durability tests (more of 5,000 h of operation): in the final stages of cell life, hydrogen

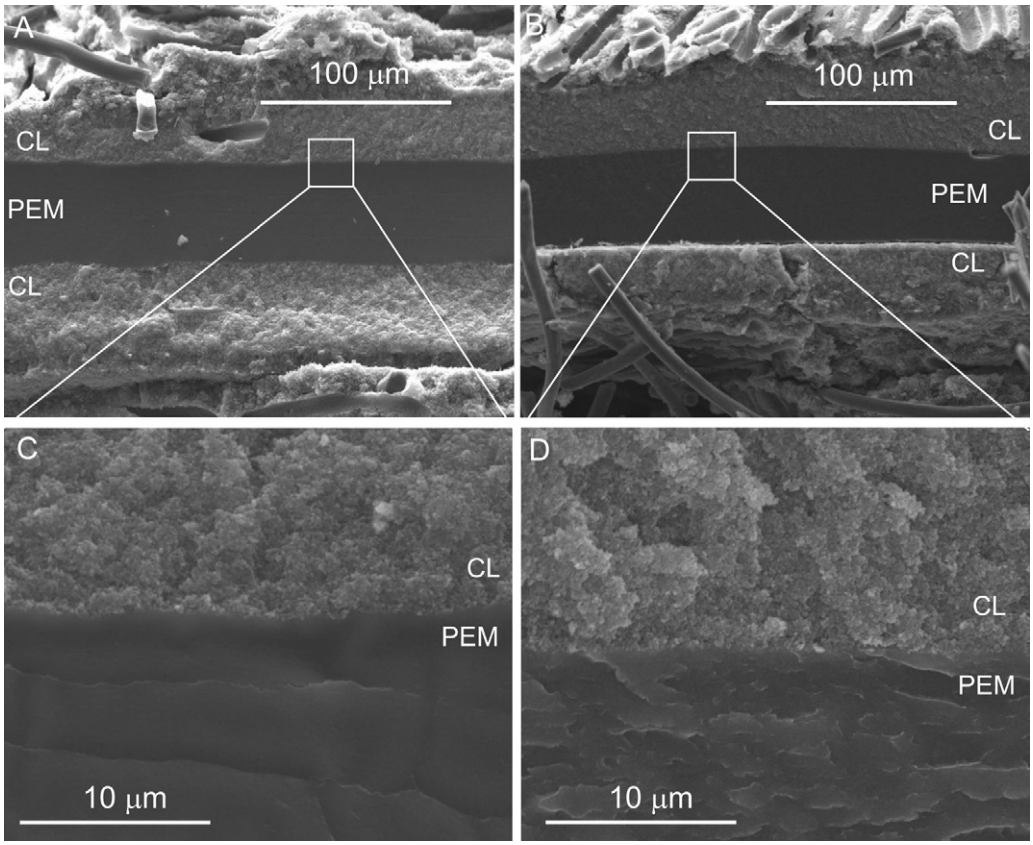

Fig. 6. SEM images of the cross-section MEAs made with Nafion® 112 MEA (A and C; magnifications 1,000× and 5,000×) and degraded Nafion® 112 MEA (B and D, magnifications 1,000× and 5,000×). Degradation was obtained by subjecting the MEA to 20 freezing/thawing cycles as described in the text (CL: catalytic layer; PEM: polymer electrolyte membrane).

crossover via such holes led to the generation of $HO^{\bullet}$ and $HO_2^{\bullet}$ radicals that accelerated membrane deterioration, resulting in the reduction of OCV. Wang et al. [19] demonstrated, via *ex situ* NMR and FTIR analysis on tested Nafion® MEAs after 96 h of operation, that the membrane degradation was originated from the decomposition of polymer main chain. With the increased loss of membrane units, small bubbles with the diameter of several microns started to form inside the membrane itself. These bubbles made the membrane vulnerable to hazards of gas crossover, which further led a catastrophic failure of the proton exchange membrane. There are mainly two ways to form hydrogen peroxide, one being oxygen reduction at the cathode [42,49], the other based on the crossover of oxygen from the cathode to the anode. The hydrogen peroxide diffuses into the membrane and reacts with metal ions, present as impurities in the membrane to form $HO^{\bullet}$ or $HOO^{\bullet}$, which can attack the polymer and degrade the membrane [50,51]. However, failure modes, especially the decay mechanism of PEMs, have not been fully understood yet.

In our recent work on PEMFCs freezing [36], we were able to partially limit the MEA damages by opportunely varying the purging procedure. Purging with dry gases during the shut-down step represents a promising approach to prevent MEA degradation [52,53]. Similar physical damages to the MEA, and to the membrane, in particular, were evidenced also by other authors during subfreezing operations. For example, Yan et al. [38], after repetitive operation below −5 °C, observed significant damage to the MEA and backing layer, catalyst layer delamination from both the membrane and the GDL, and cracks in the membrane, leading to hydrogen crossover. Alink et al. [54] reported cross-sections of MEAs with an increase in porosity and a decrease in electrode surface area after freezing/thawing cycles up to −40 °C and cold start-ups. In both cases, the membrane surface became rough and cracked and pinhole formation was observed in the membrane after operation at sub-zero temperatures. Luo et al. [55] on the contrary, reported cross-sectional SEM images of MEAs with very limited damages after various freezing/thawing cycles up to −20 °C, thanks to suitable purging procedures adopted to remove the residual water prior the shut-down of the PEMFC. But none of them reported any estimation of the hydrogen crossover rate before and/or after the repeated freezing/thawing cycles.

When the membrane is damaged after freezing/thawing cycle, the gas crossover mechanism may be completely different from the one corresponding to long term degradation under standard operating conditions. In this last case, the degradation mechanism outlined above, see, e.g., Wu et al. [11,56] may proceed through the following interconnected steps: (i) radical formation due to gas crossover, mainly at the cathode, leading to chemical degradation of the membrane; (ii) thinning of the membrane, thus increasing the gas crossover rate, and consequently the degradation of the membrane; (iii) exothermic reaction of hydrogen and oxygen at the catalyst sites leading to the formation of hotspots; (iv) local pinholes and perforation of the membrane, resulting in its dramatic irreversible degradation. Since the gas crossover rate is markedly enhanced when the cell is close to the OCV, due to higher gas pressure at the electrode's surface when hydrogen and oxygen are not removed by the electrochemical reactions, this condition is used to accelerate the degradation process, which in some cases can be recovered if steps (iii) and (iv) are not initiated [26].

In the case of the degradation produced by freezing/thawing cycles, the membrane undergoes a physical damage most probably consisting in increased micro-porosity and presence of creeps even at the beginning of its operative life. By comparing this situation to that of a fresh membrane, one of the major differences is that for the physically damaged membrane, the amount of H_2 permeating the solid layers in the membrane increases, while for the fresh membrane the preferred transport mechanism is the liquid phase. Thus for a physically damaged membrane, the amount of oxygen crossover, compared to hydrogen, cannot be neglected, resulting in a mixed potential condition also at the anode. For our degraded MEA by freezing/thawing cycle, this condition was not probably met, as indicated by the value of the hydrogen crossover current density, obtained by our method, which is two times that of a fresh MEA, but still rather small (0.73 mA cm^{-2}) compared to the values obtained at the end of long term degradation tests [56], well above 4 mA cm^{-2}.

4. Conclusions

A method for the evaluation of the hydrogen crossover current density is proposed based on the analysis of the polarization curve by means of a simplified semi-empirical model. The best fitting of the experimental data in the low current density region of the polarization curve was obtained by the assumption of a mixed potential condition for the oxygen electrode, for which the cathodic current for oxygen reduction (according to the Butler–Volmer equation) and an arbitrary parasitic oxidation current were considered. In the proposed model, the parasitic oxidation reaction is attributed to the oxidation of hydrogen crossing the membrane. For PEMFC systems, other possible oxidation reactions are negligible.

MEAs with different membranes (Nafion® 112, 115 and 117) were tested in the temperature range 60–80 °C. The hydrogen crossover current densities rose from 0.12 to 0.32 mA cm^{-2}, by decreasing the thickness of the membranes and increasing the operating cell temperatures. To confirm the applicability of the method, the hydrogen crossover determined for a fresh MEA was compared with that of a degraded one (exposed to repetitive freezing/thawing cycles). The method proved to be reliable, because, as expected, the result showed a much larger value of hydrogen crossover for the degraded MEA (more than twice the value obtained with the new one at the same temperature).

Future work will take into account other important operational parameters such as the influence of the gas pressure and ageing effects of the MEA on the hydrogen crossover current densities.

Acknowledgement

Mr Mauro Raimondo (Politecnico di Torino) is gratefully acknowledged for SEM analysis.

Appendix A. Supplementary data

Supplementary data associated with this article can be found, in the online version, at doi:10.1016/j.jpowsour.2010.09.058.

References

[1] J. Marcinkoski, J.P. Kopasz, T.G. Benjamin, Int. J. Hydrogen Energy 33 (2008) 3894–3902.
[2] R.K. Shah, in: S. Basu (Ed.), Recent Trends in Fuel Cell Science and Technology, Springer/Anamaya Publishers, New Delhi, India, 2007, pp. 1–9 (Ch. 1).
[3] L. Carrette, K.A. Friedrich, U. Stimming, Fuel Cells 1 (2001) 5–39.
[4] DoE Technical Plan, Fuel Cells (2007) 3–11, http://www.eere.energy.gov/hydrogenandfuelcells/.
[5] E. Antolini, Appl. Catal. B: Environ. 88 (2009) 1–24.
[6] E.P. Ambrosio, M.A. Dumitrescu, C. Francia, C. Gerbaldi, P. Spinelli, Fuel Cells 9 (2009) 197–200.
[7] C.W.B. Bezerra, L. Zhang, K. Lee, H. Liu, A.L.B. Marques, E.P. Marques, H. Wang, J. Zhang, Electrochim. Acta 53 (2008) 4937–4951.
[8] S. Zhang, X.Z. Yuan, J.N.C. Hin, H. Wang, K.A. Friedrich, M. Schulze, J. Power Sources 194 (2009) 588–600.
[9] W. Schmittinger, A. Vahidi, J. Power Sources 180 (2008) 1–14.
[10] A.A. Franco, M. Gerard, J. Electrochem. Soc. 155 (2008) B367–B384.
[11] J. Wu, X.Z. Yuan, J.J. Martin, H. Wang, J. Zhang, J. Shen, S. Wu, W. Merida, J. Power Sources 184 (2008) 104–109.
[12] R. Borup, J. Meyers, B. Pivovar, Y.S. Kim, R. Mukundan, N. Garland, D. Myers, M. Wilson, F. Garzon, D. Wood, P. Zelenay, K. More, K. Stroh, T. Zawodzinski, J.

Boncella, J.E. McGrath, M. Inaba, K. Miyatake, M. Hori, K. Ota, Z. Ogumi, S. Miyata, A. Nishikata, Z. Siroma, Y. Uchimoto, K. Yasuda, K. Kimijima, N. Iwashita, Chem. Rev. 107 (2007) 3904–3951.
[13] A.Z. Weber, J. Electrochem. Soc. 155 (2008) B521–B531.
[14] S. Sugawara, T. Maruyama, Y. Nagahara, S.S. Kocha, K. Shinohra, K. Tsujita, S. Mitsushima, K.-I. Ota, J. Power Sources 187 (2009) 324–331.
[15] A.B. La Conti, M. Hamdan, R.C. McDonald, in: W. Vielstich, H.A. Gasteiger, A. Lamm (Eds.), Handbook of Fuel Cells—Fundamentals, Technology and Applications, vol. 3, Fuel Cell Technology and Applications, Wiley, Chichester, UK, 2003, pp. 647–662 (Ch. 49).
[16] V.A. Sethuraman, J.W. Weidner, A.T. Haug, S. Motupally, L.V. Protsailo, J. Electrochem. Soc. 155 (2008) B50–B57.
[17] C. Chen, G. Levitin, D.W. Hess, T.F. Fuller, J. Power Sources 169 (2007) 288–295.
[18] J. Healy, C. Hayden, T. Xie, K. Olson, R. Waldo, M. Brundage, H. Gasteiger, J. Abbott, Fuel Cells 5 (2005) 302–308.
[19] F. Wang, H. Tang, M. Pan, D. Li, Int. J. Hydrogen Energy 33 (2008) 2283–2288.
[20] S. Takaichi, H. Uchida, M. Watanabe, Electrochem. Commun. 9 (2007) 1975–1979.
[21] D. Liu, S. Case, J. Power Sources 162 (2006) 521–531.
[22] J. Yu, T. Matsuura, Y. Yoshikawa, M.N. Islam, M. Hori, Electrochem. Solid State Lett. 8 (2005) A156–A158.
[23] X.-Z. Yuan, S. Zhang, H. Wang, J. Wu, J. Colin Sun, R. Hiesgen, K.A. Friedrich, M. Schulze, A. Haug, J. Power Sources 195 (2010) 7594–7599.
[24] H. Tang, S. Peikang, S. Ping Jiang, F. Wang, M. Pan, J. Power Sources 170 (2007) 85–92.
[25] S. Kundu, M. Fowler, L.C. Simon, R. Abouatallah, J. Power Sources 182 (2008) 254–258.
[26] S. Zhang, X.-Z. Yuan, J.N.C. Hin, H. Wang, J. Wu, K.A. Friedrich, M. Schulze, J. Power Sources 195 (2010) 1142–1148.
[27] M. Seddiq, H. Khaleghi, M. Mirzaei, J. Power Sources 161 (2006) 371–379.
[28] B. Sompalli, B.A. Litteer, W. Gu, H.A. Gasteiger, J. Electrochem. Soc. 154 (2007) B1349–B1357.
[29] J. Nam, P. Chippar, W. Kim, H. Ju, Appl. Energy 87 (2010) 3699–3709.
[30] S.A. Vilekar, R. Datta, J. Power Sources 195 (2010) 2241–2247.
[31] M. Inaba, T. Taro Kinumoto, M. Kiriake, R. Umebayashi, A. Tasaka, Z. Ognumi, Electrochim. Acta 51 (2006) 5746–5753.
[32] S.S. Kocha, J.D. Yang, J.S. Yi, AIChE J. 52 (2006) 1916–1925.
[33] P. Spinelli, C. Francia, E.P. Ambrosio, M. Lucariello, J. Power Sources 178 (2008) 517–524.
[34] G. Gavello, E.P. Ambrosio, U.A. Icardi, S. Specchia, C. Francia, N. Penazzi, V. Specchia, ECS Trans. 17 (2009) 359–368.
[35] G. Gavello, C. Francia, S. Specchia, U.A. Icardi, A. Graizzaro, N. Penazzi, V. Specchia, P. Spinelli, Proceedings of HFC-2009, Vancouver, BC, Canada, 31/05–03/06, 2009 (Paper # 3.402.5).
[36] G. Gavello, J. Zeng, C. Francia, U.A. Icardi, A. Graizzaro, S. Specchia, Int. J. Hydrogen Energy, HE-D-10-01007, unpublished results.
[37] E.P. Ambrosio, C. Francia, C. Gerbaldi, N. Penazzi, P. Spinelli, M. Manzoli, G. Ghiotti, J. Appl. Electrochem. 38 (2008) 1019–1027.
[38] Q. Yan, H. Toghiani, Y.W. Lee, K. Liang, H. Causey, J. Power Sources 160 (2006) 1242–1252.
[39] Y. Ishikawa, T. Morita, K. Nakata, K. Yoshida, M. Shiozawa, J. Power Sources 163 (2007) 708–712.
[40] E. Pinton, Y. Fourneron, S. Rosini, L. Antoni, J. Power Sources 186 (2009) 80–88.
[41] M.R. Tarasevich, A. Sadkowski, E. Yeager, in: B.E. Conway, J. O'M. Bockris, E. Yeager, S. Khan, R.E. White (Eds.), Comprehensive Treatise of Electrochemistry, Kinetics and Mechanism of Electrode Processes, vol. 7, Plenum Press, New York, 1983, pp. 301–398.
[42] A. Damjanovic, in: J. O'M. Bockris, B.E. Conway (Eds.), Modern Aspects of Electrochemistry, vol. 5, Plenum Press, New York, 1969, pp. 369–483.
[43] J.P. Hoare, in: P. Delahay (Ed.), Advances in Electrochemistry and Electrochemical Engineering, vol. 6, Interscience Publishers, New York, 1967, pp. 201–288.
[44] T. Akita, A. Taniguchi, J. Maekawa, Z. Siroma, K. Tanaka, M. Kohyama, K. Yasuda, J. Power Sources 159 (2006) 461–467.
[45] T.-C. Jao, S.-T. Ke, P.-H. Chi, G.-B. Jung, S.-H. Chang, Int. J. Hydrogen Energy 35 (2010) 6941–6949.
[46] Y.P. Patil, W.L. Jarrett, K.A. Mauritz, J. Membr. Sci. 356 (2010) 7–13.
[47] D. Seo, J. Lee, S. Park, J. Rhee, S.W. Choi, Y.-G. Shul, Int. J. Hydrogen Energy, in press, doi:10.1016/j.jhydene.2010.02.053.
[48] Y. Oono, T. Fukuda, A. Sounai, M. Hori, J. Power Sources 195 (2010) 1007–1014.
[49] M. Inaba, H. Yamada, J. Tokunaga, A. Tasaka, Electrochem. Solid-State Lett. 7 (2005) A474–A476.
[50] F.N. Buchi, B. Gupta, O. Haas, G.G. Scherer, Electrochim. Acta 40 (1995) 345–353.
[51] Q. Guo, P.N. Pintauro, H. Tang, S. O'Connor, J. Membr. Sci. 154 (1999) 175–181.
[52] E.A. Cho, J.-J. Ko, H.Y. Ha, S.-A. Hong, K.-Y. Lee, T.-W. Lim, I.-H. Oh, J. Electrochem. Soc. 151 (2004) A661–A665.
[53] J. Hou, B. Yi, H. Yu, L. Hao, W. Song, Y. Fu, Z. Shao, Int. J. Hydrogen Energy 32 (2007) 4503–4509.
[54] R. Alink, D. Gerteisen, M. Oszcipok, J. Power Sources 182 (2008) 175–187.
[55] M. Luo, C. Huang, W. Liu, Z. Luo, M. Pan, Int. J. Hydrogen Energy 35 (2010) 2986–2993.
[56] J. Wu, X.-Z. Yuan, J.J. Martin, H. Wang, D. Yang, J. Qiao, J. Ma, J. Power Sources 195 (2010) 1171–1176.